

Kent Academic Repository

Full text document (pdf)

Citation for published version

Pethick, Jamie and Winter, Samantha L. and Burnley, Mark (2016) Loss of knee extensor torque complexity during fatiguing isometric muscle contractions occurs exclusively above the critical torque. *American Journal of Physiology-Regulatory Integrative and Comparative Physiology*, 310 (11). R1144-R1153. ISSN 0363-6119.

DOI

<https://doi.org/10.1152/ajpregu.00019.2016>

Link to record in KAR

<http://kar.kent.ac.uk/55011/>

Document Version

Author's Accepted Manuscript

Copyright & reuse

Content in the Kent Academic Repository is made available for research purposes. Unless otherwise stated all content is protected by copyright and in the absence of an open licence (eg Creative Commons), permissions for further reuse of content should be sought from the publisher, author or other copyright holder.

Versions of research

The version in the Kent Academic Repository may differ from the final published version.

Users are advised to check <http://kar.kent.ac.uk> for the status of the paper. **Users should always cite the published version of record.**

Enquiries

For any further enquiries regarding the licence status of this document, please contact:

researchsupport@kent.ac.uk

If you believe this document infringes copyright then please contact the KAR admin team with the take-down information provided at <http://kar.kent.ac.uk/contact.html>

1 **Loss of knee extensor torque complexity during fatiguing isometric muscle**
2 **contractions occurs exclusively above the critical torque**

3

4 Jamie Pethick, Samantha L. Winter and Mark Burnley

5

6 Endurance Research Group, School of Sport and Exercise Sciences, University of Kent,
7 UK.

8

9 **Running head:** Loss of complexity above but not below the critical torque

10

11 Address for correspondence:

12 Dr Mark Burnley

13 School of Sport and Exercise Sciences

14 University of Kent

15 The Medway Building

16 Chatham Maritime

17 Kent

18 ME4 4AG

19 United Kingdom

20 m.burnley@kent.ac.uk

21

22

23

24 **Abstract**

25

26 The complexity of knee extensor torque time series decreases during fatiguing isometric
27 muscle contractions. We hypothesised that, due to peripheral fatigue, this loss of torque
28 complexity would occur exclusively during contractions above the critical torque (CT).
29 Nine healthy participants performed isometric knee extension exercise (6 s contraction,
30 4 s rest) on 6 occasions for 30 min or to task failure, whichever occurred sooner. Four
31 trials were performed above CT (trials S1-S4, S1 being the lowest intensity), and two
32 were performed below CT (at 50% and 90% of CT). Global, central and peripheral
33 fatigue were quantified using maximal voluntary contractions (MVCs) with femoral
34 nerve stimulation. The complexity of torque output was determined using approximate
35 entropy (ApEn) and the Detrended Fluctuation Analysis α scaling exponent (DFA α).
36 The MVC torque was reduced in trials below CT (by [Mean \pm SEM] $19 \pm 4\%$ in
37 90%CT), but complexity did not decrease (ApEn for 90%CT: from 0.82 ± 0.03 to 0.75
38 ± 0.06 , 95% paired-samples confidence intervals, 95% CI = $-0.23, 0.10$; DFA α from
39 1.36 ± 0.01 to 1.32 ± 0.03 , 95% CI $-0.12, 0.04$). Above CT, substantial reductions in
40 MVC torque occurred (of $49 \pm 8\%$ in S1), and torque complexity was reduced (ApEn
41 for S1: from 0.67 ± 0.06 to 0.14 ± 0.01 , 95% CI = $-0.72, -0.33$; DFA α from $1.38 \pm$
42 0.03 to 1.58 ± 0.01 , 95% CI $0.12, 0.29$). Thus, in these experiments, the fatigue-
43 induced loss of torque complexity occurred exclusively during contractions performed
44 above the CT.

45

46 **Keywords:** non-linear dynamics; fractal scaling; exercise; central and peripheral fatigue

47

48 **Introduction**

49

50 Physiological systems produce outputs that inherently fluctuate when measured over
51 time. These fluctuations in physiological time series, such as the force or torque output
52 from a contracting muscle group, can be described in terms of their *magnitude*, using
53 the standard deviation (SD) or the coefficient of variation (CV; 19, 28, 57).

54 Alternatively, such fluctuations can be quantified according to their temporal *structure*
55 or “complexity”. In this context, a complex signal has a number of characteristic
56 properties that the SD and/or spectral analysis cannot quantify, namely, temporal
57 irregularity, time irreversibility, and long-range (fractal) correlations (21, 32, 44). No
58 single statistic captures all of these properties. As a result, multiple analyses are
59 required to determine the complexity of a physiological time series (22). Measures of
60 complexity include those drawn from information theory, which quantify the regularity
61 of fluctuations in a time series (such as approximate entropy, ApEn; 43, 44), and those
62 drawn from fractal geometry, which quantify the long-range correlations present in a
63 signal (such as detrended fluctuation analysis, DFA; 39). The DFA scaling exponent, α ,
64 differentiates signals possessing white ($\alpha \sim 0.5$), pink ($\alpha \sim 1.0$), or Brownian ($\alpha \sim 1.5$)
65 noise. Using this analysis, pink noise is considered the most complex because it
66 indicates the presence of self-similar fluctuations across multiple time scales (21).
67 Complexity is thought to be a hallmark of healthy physiological systems (40). In the
68 case of the neuromuscular system, the complexity of force or torque output is thought to
69 reflect the ability to adapt motor output rapidly and accurately in response to alterations
70 in demand (31, 59).

71

72 It has been proposed that the aging process and various disease states are characterized
73 by a loss of physiological complexity (32). This “loss of complexity hypothesis”
74 initially focused on heart rate dynamics (32), but it has also been shown to apply, *inter*

75 *alia*, to respiratory frequency (41), stride timing in normal walking (24) and, crucially,
76 muscle force output (52, 56, 59). In the latter case, older adults produce less complex
77 force output during a sustained finger abduction task than young subjects, suggesting
78 that for the same relative force output motor control is diminished in older muscle (59).
79 We have recently extended the loss of complexity hypothesis to acute neuromuscular
80 system changes caused by fatigue in healthy young adults (42). In that study, repeated
81 maximal and submaximal isometric contractions of the knee extensors resulted in the
82 development of neuromuscular fatigue of both central and peripheral origin (i.e., fatigue
83 residing in the central nervous system or the muscle, respectively), assessed using
84 maximal voluntary contractions (MVCs) and supramaximal stimulation of the femoral
85 nerve (42; for review see 20). The development of fatigue was accompanied by a loss
86 of torque output complexity, measured by a progressive decrease in ApEn and a
87 progressive increase in the DFA α exponent. The mechanism producing this loss of
88 complexity is unclear, but it is well known that the mechanisms of fatigue are exercise
89 intensity dependent (45). Specifically, the mechanism responsible for peripheral
90 fatigue, as well as its rate of development, changes considerably as contractile intensity
91 is increased above the so-called critical torque (CT; 8). It is likely that the submaximal
92 contractions in our previous study (at 40% MVC) were performed above the CT, since
93 CT has been shown to occur at ~25-35% MVC using the same contraction duty cycle
94 (7, 8). Performing muscle contractions at a range of intensities straddling the CT
95 should, therefore, provide crucial insights into the fatigue-induced loss of torque
96 complexity.

97

98 The CT, analogous to the critical power frequently measured during dynamic whole-
99 body exercise such as cycling (35; for reviews, see 30, 34), represents the asymptote of
100 the hyperbolic relationship between torque output and time to task failure or
101 “exhaustion” (7, 8). Dynamic exercise performed above the critical power is associated

102 with non-steady state profiles of pulmonary O₂ uptake ($\dot{V}O_2$; 46, 47) and muscle
103 metabolism (29, 60), in contrast to the steady state profiles attainable below the critical
104 power. Similarly, below CT the neuromuscular adjustments during intermittent
105 contractions are modest (chiefly increased motor unit recruitment and/or firing
106 frequency [1, 2], reflected indirectly in the amplitude of the electromyogram [EMG]),
107 and the progression of fatigue is much slower than that during contractions performed
108 above CT (8). Above CT, there is a progressive loss of MVC torque until task failure
109 occurs, and at task failure the magnitude of peripheral fatigue is similar regardless of the
110 duration of the task (7, 8). As such, the CT represents a critical metabolic (29) and
111 neuromuscular fatigue threshold (8), and consequently metabolite-mediated peripheral
112 fatigue is thought to be the dominant mechanism of torque losses above CT (7, 8). If
113 the fatigue-induced loss of torque complexity (42) is mechanistically coupled to this
114 form of peripheral fatigue, then such a loss should only occur during contractions
115 performed above the CT. Furthermore, if the loss of complexity is related to the
116 magnitude of peripheral fatigue development above CT (rather than simply task
117 duration), then torque complexity should decrease to reach similar values at task failure,
118 regardless of the duration of exercise producing that failure.

119

120 The purpose of the present study was to investigate the effect of fatigue on the
121 complexity of knee extensor torque output in relation to the CT. To that end, we aimed
122 to determine if different temporal profiles of knee extensor torque complexity are
123 evident above and below the CT. The experimental hypothesis tested was that above the
124 CT, central and peripheral fatigue would be evident and torque complexity would be
125 progressively reduced, quantified by a decrease in ApEn and an increase in the DFA α
126 exponent, whereas below CT fatigue would develop but torque complexity would not
127 decrease.

128

129 **Materials and Methods**

130

131 *Participants*

132 Nine healthy participants (5 male, 4 female; mean \pm SD: age 25.3 ± 5.8 years; height
133 1.74 ± 0.10 m; body mass 69.2 ± 10.4 kg) provided written informed consent to
134 participate in the study, which was approved by the ethics committee of the University
135 of Kent, and which adhered to the Declaration of Helsinki. Participants were instructed
136 to arrive at the laboratory rested (having performed no heavy exercise in the preceding
137 24 hours) and not to have consumed any food or caffeinated beverages in the three
138 hours before arrival. Participants attended the laboratory at the same time of day (± 2
139 hours) during each visit.

140

141 *Experimental design*

142 Participants were required to visit the laboratory on seven occasions over a four to six
143 week period, with a minimum of 48 hours between visits. During their first visit,
144 participants were familiarized with all testing equipment and procedures, and the
145 settings for the dynamometer and stimulator were recorded. During visits two to five,
146 participants performed a series of intermittent isometric contractions to task failure
147 (“*severe trials*”; see below). From these four tests, the CT was calculated, and
148 participants subsequently performed two further tests, during visits six and seven, at
149 50% and 90% of the torque at CT (50%CT and 90%CT respectively; “*sub-CT trials*”;
150 see below) for 30 minutes or until task failure, whichever occurred first. The severe
151 trials and the sub-CT trials were each presented in a randomized order. In each trial,
152 torque output was sampled continuously to allow the quantification of complexity,
153 muscle activity was measured using the *m. vastus lateralis* electromyogram (EMG), and
154 MVCs with supramaximal femoral nerve stimulation performed before and immediately

155 after each trial were used to quantify global, central and peripheral fatigue, as detailed
156 below.

157

158 *Protocol*

159

160 *Electromyography and femoral nerve stimulation*

161 During all visits on arrival at the laboratory participants had their right leg shaved and
162 cleaned using an alcohol swab over the belly of the *vastus lateralis* and on the medial
163 aspect of the proximal tibia. For EMG acquisition, two Ag/AgCl electrodes (Nessler
164 Medizintechnik, Innsbruck, Austria) were placed on the belly of the *vastus lateralis* in
165 line with the muscle fibers, and a single electrode was placed on the medial aspect of
166 the tibia at the level of the tibial tuberosity. Care was taken to ensure that these
167 electrode locations were identical between sessions. For femoral nerve stimulation, the
168 anode (100 mm × 50 mm; Phoenix Healthcare Products Ltd, Nottingham, UK) was
169 placed on the lower portion of the right gluteus maximus lateral to the ischial tuberosity.
170 Participants then sat in the chair of a Cybex isokinetic dynamometer (HUMAC Norm;
171 CSMi, Stoughton, MA, USA), with the lever arm set so that the relative knee angle was
172 held at 90°. The chair's position was recorded and replicated in subsequent trials. The
173 position of the cathode was located using a motor point pen (Compex; DJO Global,
174 Guildford, UK), and another Ag/AgCl electrode was placed on that point. The
175 establishment of the appropriate stimulator current (200 μs pulse width) was then
176 performed as described by Pethick *et al.* (42), wherein current was incrementally
177 increased until knee extensor torque and the compound motor unit action potential (M-
178 wave) response to single twitches had plateaued and was verified during stimulation
179 delivered during a contraction at 50% MVC to ensure a maximal M-wave during was
180 also evident during an isometric contraction. The stimulator current was then increased

181 to 130% of the current producing a maximal M-wave. In all trials, doublet stimulation
182 (two 200 μ s pulses with 10 ms interpulse interval) was used.

183

184 All visits followed a similar pattern of data acquisition, beginning with the
185 instrumentation of the participants and the (re-)establishment of the correct
186 dynamometer seating position and supramaximal stimulation response. Participants then
187 performed a series of brief (3 s) MVCs to establish their maximum torque. These
188 contractions were separated by 60 s rest, and continued until three consecutive peak
189 torques were within 5% of each other. Participants were given a countdown, followed
190 by very strong verbal encouragement to maximize torque. The first MVC was used to
191 establish the fresh maximal EMG signal, against which the subsequent EMG signals
192 were normalized (*Data analysis*; see below). The second and third MVCs were
193 performed with peripheral nerve stimulation. In all instances, where MVCs were
194 performed with stimuli, the stimuli were manually delivered \sim 1.5 s into the contraction
195 to coincide with maximal torque, and 2 s after the contraction to provide a resting
196 potentiated doublet. Following the establishment of maximal torque, participants
197 rested for 10 min, and then performed either one of the severe or sub-CT trials (see
198 below). In all of these trials, at task end/failure participants immediately performed an
199 MVC, which was accompanied by peripheral nerve stimulation.

200

201 *Severe trials (performed above CT)*

202 During visit two (the first of the severe trials), the highest instantaneous pre-test
203 measure of voluntary torque was recorded as the peak MVC torque, and the target
204 torques for the submaximal contractions in visits two to five were calculated from this
205 value. The submaximal contractions were performed using a duty cycle of 0.6, with
206 contractions held for 6 s, followed by 4 s rest. The target for the submaximal
207 contractions in visit two was set at 50% of the peak torque measured in the pre-test

208 MVCs. Participants were instructed to match their instantaneous torque with a target bar
209 superimposed on the display in front of them and were required to continue matching
210 this torque for as much of the 6 s contraction as possible. The test was conducted until
211 task failure, the point at which the participant failed to reach the target torque on three
212 consecutive occasions, despite strong verbal encouragement. Participants were not
213 informed of the elapsed time during the test, but were informed of each “missed”
214 contraction. After the third missed contraction, participants were instructed to
215 immediately produce an MVC, which was accompanied by peripheral nerve
216 stimulation.

217

218 The duration of the initial severe trial at 50% MVC was used to determine the
219 percentage of MVC used in subsequent trials, which were performed in an identical
220 manner. The objective of these tests was to yield trial durations of between two and
221 fifteen minutes, which have been recommended for the assessment of CT (25). The
222 subsequent severe-intensity trials were performed in a randomized order. Visits two to
223 five were used to determine the CT; individual trials were identified as severe 1 (S1) to
224 severe 4 (S4), with S1 being the lowest and S4 being the highest torque.

225

226 *Sub-CT trials*

227 The final two visits were performed at target torques of 50% and 90% of the calculated
228 CT (identified as 50%CT and 90%CT), the order of which was determined by a coin
229 toss. These trials were conducted in the same manner as the severe trials, requiring the
230 participants to perform intermittent contractions (6 s on, 4 s off) at a target torque. In
231 these trials, the contractions continued for 30 min or until task failure, whichever
232 occurred sooner. Immediately after completion of the trial or task failure, participants
233 were instructed to perform an MVC, which was accompanied by peripheral nerve
234 stimulation. The two sub-CT trials were performed in a randomized order.

235

236

237

238 *Data acquisition and participant interface*

239 Data acquisition was performed in the same manner as described in Pethick *et al.* (42).

240 Briefly, all peripheral devices were connected via BNC cables to a Biopac MP150

241 (Biopac Systems Inc., California, USA) and a CED Micro 1401-3 (Cambridge

242 Electronic Design, Cambridge, UK) interfaced with a personal computer. All signals

243 were sampled at 1 kHz. The data were collected in Spike2 (Version 7; Cambridge

244 Electronic Design, Cambridge, UK). A chart containing the instantaneous torque was

245 projected onto a screen placed ~1 m in front of the participant. A scale consisting of a

246 thin line (1 mm thick) was superimposed on the torque chart and acted as a target, so

247 that participants were able to match their instantaneous torque output to the target

248 torque during each test.

249

250 *Data analysis*

251 All data were processed and analyzed using code written in MATLAB R2013a (The

252 MathWorks, Massachusetts, USA).

253

254 *Torque and EMG.* The mean and peak torque for each contraction in every test was

255 determined. The mean torque was calculated based on the steadiest five seconds of each

256 contraction. The torque impulse (the integral of torque and time) was also calculated for

257 each contraction. The EMG signal from the *vastus lateralis* was filtered (10-500 Hz)

258 full-wave rectified with a gain of 1000. The average rectified EMG (arEMG) for each

259 contraction was then calculated and normalized by expressing the arEMG as a fraction

260 of the arEMG obtained during an MVC from the fresh muscle performed at the

261 beginning of each trial.

262

263 To determine task failure, the mean contraction torque produced in the first minute of
264 the contractions was calculated, and task failure was deemed to have occurred when
265 participants' mean torque output failed to achieve that in the first minute by more than 5
266 N.m for three consecutive contractions, with the first of these contractions being the
267 time at which task failure occurred. To determine the CT, the total torque impulse
268 produced until task failure and the total contraction time during each individual trial
269 were calculated. The torque impulse was then plotted against the contraction time, and
270 the parameters of the torque-duration relationship were estimated using linear regression
271 of the torque impulse vs. contraction time (7, 8):

272

$$273 \text{ Torque impulse} = W' + CT \cdot t \quad [1]$$

274

275 where W' represents the curvature constant parameter and t is the time to task failure.

276

277 *Central and peripheral fatigue.* Measures of central and peripheral fatigue were
278 calculated based on the stimuli delivered during and after pre-test and task failure
279 MVCs. Global fatigue was assessed using the fall in the MVC torque, peripheral
280 fatigue was evidenced by a fall in the peak potentiated doublet torque, and central
281 fatigue by the decline in voluntary activation (VA; 5):

282

$$283 VA = 1 - (\text{superimposed doublet/potentiated doublet}) \times 100 \quad [2]$$

284

285 The time to peak torque and the half-relaxation time were also calculated from each
286 resting potentiated doublet. The time to peak torque was measured as the time from the
287 delivery of the stimulus to the highest torque response, and the half-relaxation time was
288 measured as half the time from the peak torque to the recovery of baseline torque. In

289 one participant during the CT50% trial, the stimulator failed to deliver a doublet
290 stimulus and the doublet data from that test were not used in the analysis.

291

292 *Variability and complexity.* All measures of variability and complexity were calculated
293 using the steadiest five seconds of each contraction, identified as the 5 seconds
294 containing the lowest standard deviation (SD). The amount of variability in the torque
295 output of each contraction was measured using the SD, which provides a measure of the
296 absolute amount of variability in a time series and coefficient of variation (CV), which
297 provides a measure of the amount of variability in a time series normalized to the mean
298 of the time series. Force accuracy was quantified by calculating the root mean squared
299 error (RMS error) between the target torque and the instantaneous torque during the
300 steadiest 5 seconds of each contraction.

301

302 The temporal structure, or complexity, of torque output was then examined using
303 multiple time domain analyses. To determine the regularity of torque output, we
304 calculated ApEn (43), and to estimate the temporal fractal scaling of torque detrended
305 fluctuation analysis (DFA) was used (39). Sample entropy was also calculated (48), but
306 as shown in Pethick *et al.* (42) this measure did not differ from ApEn, and was not
307 included in the present analysis. As detailed in Pethick *et al.* (42), ApEn was calculated
308 with the template length, m , set at 2 and the tolerance, r , set at 10% of the standard
309 deviation of torque output, and DFA was calculated across time scales (57 boxes
310 ranging from 1250 to 4 data points).

311

312 *Statistics*

313 All data are presented as means \pm SEM. Two-way ANOVAs with repeated measures
314 were used to test for differences between conditions and time points, and for a
315 condition*time interaction for torque, arEMG, potentiated doublet torque, voluntary

316 activation, variability and complexity. The variability and complexity measures were
317 analyzed using means from the first minute and the final minute before task end/failure.
318 The rates of change in all parameters were analyzed using one-way ANOVAs with
319 repeated measures. Main effects were considered significant when $P < 0.05$. When
320 main effects were observed, Bonferroni-adjusted 95% paired-samples confidence
321 intervals were then used to determine specific differences.

322

323

324 **Results**

325

326 *Preliminary measures and the CT*

327 The peak instantaneous MVC torque recorded during an MVC in visit two was $198.1 \pm$
328 17.2 N.m. This was used to set the target torques for the four tests performed above CT,
329 which ranged from 78.7 ± 6.3 to 112.7 ± 9.0 N.m, or 40.8 ± 2.6 to $57.8 \pm 2.5\%$ MVC
330 (Table 1). The CT was calculated to be 57.5 ± 4.7 N.m, which was equivalent to $29.7 \pm$
331 1.7% MVC, and the W' was 3637 ± 537 N.m.s. The 95% CI for the estimation of CT
332 was 11.8 ± 2.3 N.m. The two trials below CT (50%CT and 90%CT) were performed at
333 28.7 ± 2.3 and 51.7 ± 4.2 N.m, or 14.9 ± 0.9 and $26.7 \pm 1.6\%$ MVC, respectively (Table
334 1).

335

336 *Torque and EMG*

337 For the trials above the CT, task failure occurred when participants were no longer able
338 to achieve the target torque, despite a maximal effort. All trials above the CT resulted in
339 significant decreases in MVC torque ($F = 62.17$, $P < 0.001$), with the mean MVC torque
340 at task failure being not significantly different from (S1-S3) or significantly lower than
341 (S4) the torque produced during the submaximal contractions (Table 1). In contrast, all
342 participants completed 30 minutes of contractions in both trials below the CT. At the
343 end of these trials, the mean MVC torque was still significantly greater than the
344 submaximal torque requirements (paired-samples confidence intervals (CIs): 90%CT,
345 52.6 , 168.2 N.m; 50%CT, 92.2 , 211.3 N.m), indicating that contractions performed
346 below the CT ended with a substantial reserve in maximal torque.

347

348 The arEMG amplitude increased over time in all of the trials above the CT, reaching
349 ~ 61 - 77% of the pre-test MVC value at task failure ($F = 14.33$, $P = 0.005$; Table 1).

350 Contractions below the CT resulted in only modest increases in arEMG as the trials

351 progressed, with the values at task end not significantly different from those at the start
352 (CIs: 90%CT, -4.7, 19.0%; 50%CT, -0.6, 2.9%).

353

354 *Peripheral and central fatigue*

355 All the trials above the CT resulted in significant reductions in potentiated doublet
356 torque ($F = 34.34$, $P = 0.001$; Table 1), indicating the presence of peripheral fatigue.
357 The potentiated doublet torque attained at task failure was not significantly different
358 between trials above CT (CIs: S1 vs. S2 -19.2, 20.5 N.m; S1 vs. S3, -10.9, 12.4 N.m;
359 S1 vs. S4, -11.9, 17.2 N.m; Table 1). The time to peak tension ($F = 2.85$, $P = 0.15$) and
360 half-relaxation time ($F = 0.34$, $P = 0.62$) were unaffected by contractions above CT.
361 Voluntary activation significantly declined during all trials above the CT ($F = 192.21$, P
362 < 0.001 ; Table 1), indicating the presence of central fatigue. The potentiated doublet
363 torque was reduced in both trials below CT, but not to the same extent as trials above
364 CT (Table 1). Voluntary activation also significantly decreased in 90%CT (CI: -9.4, -
365 1.7%). There was no change in voluntary activation during contractions at 50%CT (CI:
366 -5.9, 3.5%).

367

368 *Variability and complexity*

369 The variability and complexity data are presented in Table 2. All trials above the CT
370 resulted in a significant increase in the amount of variability, as measured by the SD (F
371 $= 110.15$, $P < 0.001$) and CV ($F = 136.96$, $P < 0.001$). The values attained at task failure
372 for the SD were not significantly different across trials above CT. The trials below the
373 CT resulted in no change in the amount of variability (SD CIs: 90%CT, -0.1, 0.7 N.m;
374 50%CT, -0.1, 0.5 N.m; CV: 90%CT, -0.2, 1.5%; CT50%, -0.1, 2.0%), and the values
375 at task end were significantly lower than those at task failure in the trials above the CT
376 (Table 2). Force accuracy was higher in the CT50% and CT90% trials than in S1 ($F =$

377 23.06, $P < 0.001$), and accuracy declined only during contractions performed above the
378 CT ($F = 101.5$, $P < 0.001$, Table 2).

379

380 Complexity at the beginning of the trials decreased with increasing torque requirements
381 from 50%CT to S4 (ApEn, $F = 35.54$, $P < 0.001$; DFA α , $F = 38.97$, $P < 0.001$; Figure
382 1). Representative time series of torque output during contractions below and above CT
383 are shown in Figure 2. All trials above the CT resulted in decreases in complexity, as
384 measured by ApEn ($F = 192.30$, $P < 0.001$) and DFA α ($F = 46.28$, $P < 0.001$; Figure 2;
385 Figure 3). ApEn decreased as the trials progressed, with the values at task failure in S1-
386 S4 being similar, despite different starting values (Table 2; Figure 1A). DFA α
387 increased, indicating more Brownian-like noise, as the trials progressed, with no
388 significant differences between trials for the values at task failure. In contrast, the trials
389 below the CT resulted in no significant change in complexity after 30 min of
390 contractions: ApEn CIs, 90%CT, -0.23 , 0.10 ; 50%CT, -0.29 , 0.05 ; DFA α CIs 90%CT,
391 -0.12 , 0.04 ; 50%CT, -0.06 , 0.11 . At the end of these tasks the values were significantly
392 higher (ApEn) or lower (DFA α) than at task failure above CT (Table 2; Figure 1B;
393 Figure 3).

394

395 *Rates of fatigue development*

396 The rates of decrease in MVC torque, potentiated doublet torque and voluntary
397 activation all increased with increasing torque requirements from 50%CT to S4 and
398 were significantly greater above compared to below the CT (MVC, $F = 34.41$, $P <$
399 0.001 ; potentiated doublet, $F = 16.68$, $P = 0.002$; voluntary activation, $F = 17.71$, $P =$
400 0.001 ; Table 1). The rate of increase in arEMG also increased with increasing torque
401 requirements and was significantly greater above compared to below the CT ($F = 8.63$,
402 $P = 0.008$; Table 1).

403

404 The rate of decrease in ApEn (Figure 4A) increased with increasing torque requirements
405 from 90%CT to S4 and was significantly greater above compared to below the CT
406 (ApEn, $F = 34.94$, $P < 0.001$; Table 2). The rate of increase in DFA α (Figure 4B)
407 increased with increasing torque requirements from 90%CT to S4 and was significantly
408 greater above compared to below the CT ($F = 14.52$, $P = 0.001$; Table 2).

409

410 **Discussion**

411

412 The major novel finding of this investigation was that the complexity of knee extensor
413 torque output was reduced during contractions performed exclusively above the critical
414 torque. Contractions performed above CT were associated with the development of
415 substantial central and peripheral fatigue, accompanied by reduced complexity and
416 increasingly Brownian (DFA $\alpha = 1.50$) fluctuations in torque output. At task failure
417 above CT, torque complexity, voluntary activation and the potentiated doublet torque all
418 fell to reach similar values regardless of the torque requirement of the task. In contrast,
419 contractions below the CT resulted in no change in the complexity of torque output, in
420 spite of the development of peripheral fatigue (at 50% and 90%CT) and central fatigue
421 (at 90%CT). These results provide new evidence that torque complexity is sensitive to
422 the development of neuromuscular fatigue only during high-intensity (>CT) voluntary
423 contractions.

424

425 *Effect of fatigue on the magnitude of torque fluctuations: variability vs. complexity*

426 The contractions performed above the CT led to a marked increase in the SD, CV and
427 RMS error of torque fluctuations, whereas contractions below the CT did not (Table 2).
428 A fatigue-induced increase in the amplitude of torque fluctuations during isometric
429 contractions has been repeatedly observed (10, 18, 26). Whilst a progressive increase in
430 the amplitude of torque fluctuations mirrors the loss of torque output complexity, it is

431 important to appreciate that measures of complexity quantify different properties of the
432 torque signal (31). Specifically, the ApEn statistic quantifies regularity by identifying
433 template matches in a time series, with fewer matches indicating greater complexity,
434 and the DFA α exponent identifies noise color and, if present, long-range correlations.
435 The DFA α exponent increasing above unity towards ~ 1.5 (as seen the present study)
436 also indicates a less complex, Brownian noise-like signal. Crucially, changes in time
437 series complexity can be observed in the absence of changes in the magnitude of
438 fluctuations (i.e., the SD), as reported, for example, in postural tremor in Parkinson's
439 patients (58). Thus, the temporal structure of physiological time series contains
440 information additional to, and distinct from, amplitude-based measures of time series
441 variability (32).

442

443 *Neuromuscular fatigue and complexity below and above the critical torque*

444 The fatigue-induced loss of torque complexity we previously reported was observed
445 during either a series of MVCs or contractions performed at 40% MVC to task failure
446 (42). By utilizing a broad range of target torques in the present study (from ~ 15 -60%
447 MVC), we aimed to examine whether the fatigue-induced loss of complexity was
448 dependent on contractile intensity, with specific reference to the CT. Although the
449 critical power (or torque) was originally proposed to represent a power (or torque)
450 below which fatigue would not occur (34), it is now known that fatigue does develop
451 below the CT, but at a disproportionately slower rate than above CT (8). The results of
452 the present study support this, with the decrease in MVC torque occurring more than
453 four times faster for the S1 trial compared to the 90%CT trial, and with the rate of
454 fatigue in all its forms increasing as the torque demands increased above CT (Table 1).
455 It is thought that the dominant mechanism of fatigue above CT is metabolite-induced
456 peripheral fatigue (7, 8), on the basis that progressive phosphorylcreatine (PCr)
457 depletion and phosphate (P_i) and H^+ accumulation only occur above the CT (29, 60). P_i

458 accumulation, in particular, has been associated with fatigue in skinned fiber
459 preparations (15, 37), either through a direct effect on crossbridge force (12, 38), or
460 through depressive effects on Ca^{2+} kinetics (15). Recently, it has also been suggested
461 that the effects of P_i and H^+ accumulation are additive (36), resulting in profound
462 peripheral fatigue during high-force contractions. The loss of muscle force-generating
463 capacity *in vivo* results in additional motor unit recruitment to sustain the demands of
464 the task (1, 2), reflected, albeit indirectly, by an increase in *vastus lateralis* EMG
465 amplitude (Table 1). Collectively, these metabolic and neuromuscular responses drive
466 the non-steady state increases in muscle and pulmonary $\dot{\text{V}}\text{O}_2$ that occur above the
467 critical power/torque (46, 49, 61). As a result, neuromuscular fatigue above critical
468 power leads to a progressive decrease in muscular efficiency (23).

469

470 The present investigation adds a further dimension to the critical power concept,
471 because for the first time we show that the fatigue-induced loss of torque output
472 complexity we previously reported (42) occurs only above the CT. Specifically, above
473 the CT the ApEn statistic decreased (indicating increased signal regularity) and the DFA
474 α exponent increased towards values approximating Brownian noise (~ 1.5 , Table 2,
475 Figures 2 and 3). Both metrics indicate a progressive reduction in the complexity of the
476 torque signal as fatigue develops above, but not below, CT. The factors that link this
477 loss of complexity with CT are not clear, but Seely and Macklem (50) have
478 hypothesized a link between a system's prevailing metabolic rate and its output
479 complexity. Our results support this hypothesis, since it is only above the CP/CT that
480 muscle $\dot{\text{V}}\text{O}_2$ rises inexorably as a function of time, and we show here that complexity
481 only falls as a function of time above CT. Thus, it is possible that the loss of
482 complexity observed in the present study is linked to the distinct metabolic,
483 neuromuscular and respiratory perturbations that occur above the critical power/torque.

484

485 Despite the lack of change in complexity during contractions below the CT, a modest
486 degree of global, central and peripheral fatigue was nevertheless observed in these
487 conditions (Table 1). Specifically, by the end of the task in both the 50%CT and 90%CT
488 trials, the potentiated doublet torque had declined, and at 90%CT the voluntary
489 activation had decreased. This suggests that complexity is dissociated from the
490 development of central and peripheral fatigue below the CT, and that fatigue
491 mechanisms particular to contractions above CT are responsible for the loss of
492 complexity we observed. Below CT, the responses of PCr, P_1 and pH to exercise (29)
493 are probably too small to affect the neuromuscular system's submaximal output to any
494 significant degree. Thus, the neuromuscular system's freedom to explore and achieve
495 control solutions (i.e., its "adaptability", reflected by its output complexity; 31, 40, 51,
496 59) is not significantly perturbed and contractions continue with relative ease. These
497 results considerably advance our previous findings on both neuromuscular fatigue (8)
498 and torque complexity (42) in that they demonstrate that metrics derived from the field
499 of non-linear dynamics can be used to identify changes in neuromuscular system
500 behavior coincident with the CT.

501

502 *Physiological bases for changes in torque complexity above critical torque*

503 During fatiguing submaximal contractions, the neuromuscular system must maintain the
504 torque output in the face of reduced muscle fiber twitch forces (3) and motoneurone
505 excitability (33), by increasing central drive and thus motor unit recruitment and rate
506 coding (1, 6, 14). As the fatiguing contractions progress, therefore, a greater pool of
507 fibers is engaged in the task, but due to peripheral fatigue each fiber contributes
508 progressively less to the torque output. The net effect of this would likely be a
509 smoothing of the torque time series, and thus reduced torque complexity (Figures 2 and
510 3; 42). Although we observed no change in the time to peak tension or the half-
511 relaxation time in response to doublet stimulation of the femoral nerve (Table 1), a

512 slowing of these responses has been reported previously (9, 27) and could, if present,
513 also contribute to a smoothing of the torque time series. That the fatigue-induced loss
514 of complexity appears to occur exclusively above the CT (at least for tasks lasting 30
515 min or less) is crucial, because it suggests that only metabolite-mediated peripheral
516 fatigue is capable of commencing the chain of events leading to the loss of torque
517 complexity. These events seem to include both peripheral alterations and the central
518 adjustments required to counter them in order to continue exercise.

519

520 One of the central adjustments that may be key to the fatigue-induced loss of
521 complexity is the common synaptic input to motoneurons and the modulation of motor
522 unit discharge rates (i.e., common drive; 13, 16). A necessary consequence of a
523 common synaptic input to all motoneurons is the correlated discharge of action
524 potentials, known as motor unit synchronization (16). It has recently been demonstrated
525 that there is an increase in common synaptic input when the net excitatory input to
526 motoneurons increases, whether this is due to an increase in contraction intensity or to
527 the progression of fatigue and the necessary recruitment of a greater proportion of the
528 motor unit pool (11). The fatiguing contractions performed in Castronovo *et al.* (20-
529 75% MVC; 11) were likely to have been above the “critical force” for the tibialis
530 anterior, since critical force typically occurs at ~15% MVC for sustained contractions
531 (34). The present study demonstrates that both increased contractile intensity and
532 neuromuscular fatigue are also associated with decreased torque output complexity
533 (Figure 1, Table 2). Consequently, if common synaptic input explains most of the
534 variance in torque fluctuations (16, 17), then our results imply that fatigue processes
535 may influence the temporal complexity of common synaptic input and thus neural drive
536 to the muscle (17). However, the EMG measurements made in the present study (using
537 a single set of bipolar surface electrodes) did not allow us to address this hypothesis.
538 Nevertheless, common synaptic input oscillating at a single dominant frequency has

539 been suggested to cause the increased regularity of loaded postural tremor with aging
540 (55).

541

542 As we have previously observed (8), peripheral fatigue developed more than four times
543 faster above than below CT, and its rate of development accelerated as the torque
544 requirements increased above CT (Figure 4B; Table 1). At task failure, however, the
545 potentiated doublet had declined to similar levels, regardless of its rate of change or the
546 intensity of the contractions themselves (Table 1). This is consistent with previous data
547 demonstrating a consistent level of metabolic disturbance and/or peripheral fatigue at
548 task failure (4, 8, 60). A major novel finding of the present investigation was that at
549 task failure the values of ApEn and DFA α were similar for each of the trials above the
550 CT, regardless of their starting values and their rate of change during the trials (Table
551 2). This indicates that task failure is characterized not only by consistent levels of
552 metabolic disturbance and peripheral fatigue, but also by consistently low levels of
553 torque complexity (Figure 1). Whether low complexity torque output plays a direct role
554 in precipitating task failure is not presently clear (42). Nevertheless, a high level of
555 physiological complexity is thought to be advantageous because it endows
556 physiological systems with the ability to rapidly adapt to sudden changes in demand
557 (31, 32, 40, 54). A loss of motor output complexity is associated with diminished motor
558 control in aging (53-55, 59). In the present study, the high-frequency fluctuations
559 present at the beginning of the trials above CT were progressively attenuated as task
560 failure approached, giving way to large, low-frequency fluctuations (Figure 2B). These
561 patterns are a signature of the neuromuscular system becoming unable to consistently
562 match the target demand (54). At task failure, torque complexity reached consistently
563 low values that may have compromised motor control and therefore limited task
564 performance, in agreement with the purported functional importance of physiological
565 complexity (31, 40, 54, 59). Thus, a role for low torque complexity in the mechanism

566 of task failure is plausible, but further studies are required to directly test this
567 hypothesis.

568

569

570 *Perspectives and Significance*

571 The loss of torque complexity that occurred during fatiguing contractions above the CT
572 in this study extends the “loss of complexity hypothesis” developed in aging and disease
573 (32) to high-intensity (>CT) contractions in young healthy participants. Exploration of
574 the central and peripheral mechanisms of this loss of torque complexity should,
575 therefore, center on muscle contractions performed above the CT. The loss of
576 complexity observed above CT implies that adaptability of the neuromuscular system is
577 progressively compromised, which likely contributes to the processes resulting in task
578 failure. Whether the fatigue-induced loss of complexity occurs when the target torque is
579 varied (during sinusoidal or ramp-and-hold contractions, for example; 1, 59), or when
580 dynamic contractions are performed in tasks such as cycling, is not clear. Establishing
581 the effect of fatigue on neuromuscular output complexity in a range of tasks, and
582 establishing the central and peripheral processes involved are, therefore, important next
583 steps. Given the development of wearable or equipment-mounted devices to measure
584 neuromuscular output during exercise, such work could pave the way to real-time
585 assessment of the fatigue process in free running conditions.

586

587 **Disclosures:**

588

589 This work was supported by a University of Kent 50th Anniversary Scholarship. No
590 external funding was received for this work. The authors report no conflicts of interest,
591 financial or otherwise.

592

593 **Figure legends**

594

595 **Figure 1**

596 **Relationship between knee extensor torque requirement and torque complexity**

597 Panel A shows the approximate entropy measured in the first minute and in the last
598 minute of each intermittent contraction trial. Panel B shows the DFA α scaling
599 exponent measured in the same trials as panel A. Each trial (50%CT, 90%CT, S1-S4) is
600 highlighted between the two panels. CT occurred at $29.7 \pm 1.7\%$ MVC. Note that
601 complexity is significantly decreased (as shown by reduced ApEn and increased DFA α
602 exponent) only during contractions above the CT (white triangles). All values are mean
603 \pm SEM.

604

605 **Figure 2**

606 **Responses of knee extensor torque during representative contractions below and**
607 **above the critical torque**

608 Panel A shows three contractions from the 90%CT trial in a representative participant:
609 one in the first minute (3rd contraction), one at the mid-point (90th contraction), and one
610 at the end of the task (180th contraction). Notice that there is no change in the measures
611 of torque complexity as contractions progress. The amplitude of fluctuations appear
612 greater at the mid-point and at the end of the task by virtue of a slightly larger SD in
613 these contractions (1.4, 1.8, and 1.9 N.m, in first minute, mid-point and task end,
614 respectively). In panel B, data are taken from a test performed at 50% MVC (S3 trial),
615 in which task failure occurred in 3 min 50 s. The first minute is represented by the 2nd
616 contraction of the test, the mid-point by the 12th contraction (2 min) and task failure by
617 the 22nd contraction (immediately preceding task failure). Notice the progressive loss of
618 torque complexity in each contraction (shown by the decreased ApEn and increased
619 DFA α exponent).

620

621 **Figure 3**

622 **Time course of complexity in response to contractions below and above the critical**
623 **torque**

624 Panel A shows approximate entropy (ApEn), Panel B shows the Detrended Fluctuation
625 Analysis α scaling exponent (“DFA α exponent”). In each panel, the white circles
626 represent the 90%CT trial (below CT) and the black circles the S1 trial (the lowest
627 torque performed above CT). Note the progressive decrease in ApEn and the
628 progressive increase in the DFA α exponent during contractions above the CT, with no
629 change during contractions below the CT. All values are mean \pm SEM.

630

631 **Figure 4**

632 **Rate of change in torque complexity in relation to torque requirements**

633 Panels A and B show the rate of change in ApEn and the DFA α exponent, respectively.
634 White circles, trials below CT; black symbols, trials above CT. Note that the rates of
635 change for all variables are different from zero only above CT, and these rates increase
636 as torque requirements are increased above CT. All values are mean \pm SEM.

637

638

639 **References**

640

641 1. **Adam A, De Luca CJ.** Recruitment order of motor units in human vastus lateralis
642 muscle is maintained during fatiguing contractions. *J Neurophysiol* 90: 2919-2927,
643 2003.

644

645 2. **Adam A, De Luca CJ.** Firing rates of motor units in human vastus lateralis muscle
646 during fatiguing isometric contractions. *J Appl Physiol* 99: 268-280, 2005.

647

648 3. **Allen DG, Lamb GD, Westerblad H.** Skeletal muscle fatigue: cellular mechanisms.
649 *Physiol Rev* 88: 287-332, 2008.

650

651 4. **Amann M, Romer LM, Subudhi AW, Pegelow DF, Dempsey JA.** Severity of
652 arterial hypoxaemia affects the relative contributions of peripheral muscle fatigue to
653 exercise performance in humans. *J Physiol* 581: 389-403, 2007.

654

655 5. **Behm DG, St-Pierre DMM, Perez D.** Muscle inactivation: assessment of
656 interpolated twitch technique. *J Appl Physiol* 81: 2267-2273, 1996.

657

658 6. **Bigland-Ritchie B, Furbush F, Woods JJ.** Fatigue of intermittent submaximal
659 voluntary contractions: central and peripheral factors. *J Appl Physiol* 61: 421-429, 1986.

660

661 7. **Burnley M.** Estimation of critical torque using intermittent isometric maximal
662 voluntary contractions of the quadriceps in humans. *J Appl Physiol* 106: 975-983, 2009.

663

- 664 8. **Burnley M, Vanhatalo A, Jones AM.** Distinct profiles of neuromuscular fatigue
665 during muscle contractions below and above the critical torque in humans. *J Appl*
666 *Physiol* 113: 215-223, 2012.
- 667
- 668 9. **Cady EB, Elshove H, Jones DA, Moll A.** The metabolic causes of slow relaxation
669 in fatigued human skeletal muscle. *J Physiol* 418: 327-337, 1989.
- 670
- 671 10. **Contessa P, Adam A, De Luca CJ.** Motor unit control and force fluctuation during
672 fatigue. *J Appl Physiol* 107: 235-243, 2009.
- 673
- 674 11. **Castronovo AM, Negro F, Conforto S, Farina D.** The proportion of synaptic input
675 to motor neurons increases with an increase in net excitatory input. *J Appl Physiol* 119:
676 1337-1346, 2015.
- 677
- 678 12. **Debold EP, Romatowski J, Fitts RH.** The depressive effect of Pi on the force-pCa
679 relationship in skinned single muscle fibers is temperature dependent. *Am J Physiol Cell*
680 *Physiol* 290: C1041-50, 2006.
- 681
- 682 13. **De Luca CJ, Erim Z.** Common drive of motor units in regulation of muscle force.
683 *Trends Neurosci*, 17: 299-305, 1994.
- 684
- 685 14. **Dideriksen JL, Enoka RM, Farina D.** Neuromuscular adjustments that constrain
686 submaximal EMG amplitude at task failure of sustained isometric contractions. *J Appl*
687 *Physiol* 111, 485-494, 2011.
- 688

- 689 15. **Dutka TL, Cole L, Lamb GD.** Calcium phosphate precipitation in the
690 sarcoplasmic reticulum reduces action potential-mediated Ca^{2+} release in mammalian
691 skeletal muscle. *Am J Physiol Cell Physiol* 289: C1502-C1512, 2005.
692
- 693 16. **Farina D, Negro F.** Common synaptic input to motor neurons, motor unit
694 synchronization and force control. *Exerc Sport Sci Rev* 43: 23-33, 2015.
695
- 696 17. **Farina D, Negro F, Dideriksen JL.** The effective neural drive to muscles is the
697 common synaptic input to motor neurons. *J Physiol* 592: 3427-3441, 2014.
698
- 699 18. **Furness P, Jessop J, Lippold OCJ.** Long-lasting increases in the tremor in human
700 hand muscles following brief, strong effort. *J Physiol* 265: 821-831, 1977.
- 701 19. **Galganski ME, Fuglevand AJ, Enoka RM.** Reduced control of motor output in a
702 human hand muscle of elderly participants during submaximal contractions. *J*
703 *Neurophysiol* 69: 2108-2115, 1993.
704
- 705 20. **Gandevia SC.** Spinal and supraspinal factors in human muscle fatigue. *Physiol Rev*
706 81: 1725-1789, 2001.
707
- 708 21. **Goldberger AL, Amaral LAN, Hausdorff JM, Ivanov PC, Peng CK, Stanley**
709 **HE.** Fractal dynamics in physiology: Alterations with disease and aging. *Proc Nat Acad*
710 *Sci* 99: 2466-2472, 2002.
711
- 712 22. **Goldberger AL, Peng C-K, Lipsitz LA.** What is physiologic complexity and how
713 does it change with aging and disease? *Neurobiol Aging* 23: 23-26, 2002.
714

715 23: **Grassi B, Rossiter HB, Zoladz JA.** Skeletal muscle fatigue and decreased
716 efficiency: two sides of the same coin? *Exerc Sport Sci Rev* 43: 75-83, 2015.
717

718 24. **Hausdorff JM, Mitchell SL, Firtion R, Peng CK, Cudkowicz ME, Wei JY,**
719 **Goldberger AL.** Altered fractal dynamics of gait: reduced stride-interval correlations
720 with aging and Huntington's disease. *J Appl Physiol* 82: 262-269, 2001.
721

722 25. **Hill DW.** The critical power concept: A review. *Sports Med* 16: 237-254, 1993.
723

724 26. **Hunter SK, Enoka RM.** Changes in muscle activation can prolong the endurance
725 time of a submaximal isometric contraction in humans. *J Appl Physiol* 94: 108-118,
726 2003.
727

728 27. **Jones DA, Turner DL, McIntyre DB, Newham DJ.** Energy turnover in relation to
729 slowing of contractile properties during fatiguing contractions of the human anterior
730 tibialis muscle. *J Physiol* 587: 4329-4338, 2009.
731

732 28. **Jones KE, Hamilton AFDC, Wolpert DM.** Sources of signal-dependent noise
733 during isometric force production. *J Neurophysiol* 88: 1533-1544, 2002.
734

735 29. **Jones AM, Wilkerson DP, DiMenna F, Fulford J, Poole DC.** Muscle metabolic
736 responses to exercise above and below the "critical power" assessed using ³¹P-MRS. *Am*
737 *J Physiol Regul Integr Comp Physiol* 294: R585-R593, 2008.
738

739 30. **Jones AM, Vanhatalo A, Burnley M, Morton RH, Poole DC.** Critical power:
740 implications for the determination of $\dot{V}O_2$ max and exercise tolerance. *Med Sci Sports*
741 *Exerc* 42: 1876-1890, 2010.

742

743 31. **Lipsitz LA.** Dynamics of stability: the physiologic basis of functional health and
744 frailty. *J Gerontol A Biol Sci Med Sci* 57A: B115-B125, 2002.

745

746 32. **Lipsitz LA, Goldberger AL.** Loss of ‘complexity’ and aging: Potential applications
747 of fractals and chaos theory to senescence. *JAMA* 267: 1806-1809, 1992.

748

749 33. **McNeil CJ, Giesebrecht S, Gandevia SC, Taylor JL.** Behaviour of the
750 motoneurone pool in a fatiguing submaximal contraction. *J Physiol* 589: 3533-3544,
751 2011.

752

753 34. **Monod H, Scherrer J.** The work capacity of a synergic muscular group.
754 *Ergonomics* 8: 329-338, 1965.

755

756 35. **Moritani T, Nagata A, deVries HA, Muro M.** Critical power as a measure of
757 physical work capacity and anaerobic threshold. *Ergonomics* 24: 339-350, 1981.

758

759 36. **Nelson CR, Fitts RH.** Effects of low cell pH and elevated inorganic phosphate on
760 the pCa-force relationship in single muscle fibers at near-physiological temperatures.
761 *Am J Physiol Cell Physiol* 306: C670-C678, 2014.

762

763 37. **Nosek TM, Fender KY, Godt RE.** It is diprotonated inorganic phosphate that
764 depresses force in skinned skeletal muscle fibers. *Science* 236: 191-193, 1987.

765

766 38. **Palmer S, Kentish JC.** The role of troponin C in modulating the Ca²⁺ sensitivity of
767 mammalian skinned cardiac and skeletal muscle fibres. *J Physiol* 480: 45-60, 1994.

768

- 769 39. **Peng C-K, Buldyrev SV, Havlin S, Simon M, Stanley HE, Goldberger AL.**
770 Mosaic organization of DNA nucleotides. *Phys Rev E* 49: 1685-1689, 1994.
771
- 772 40. **Peng C-K, Costa M, Goldberger AL.** Adaptive data analysis of complexity
773 fluctuations in physiologic time series. *Adv Adapt Data Anal* 1: 61-70, 2009.
774
- 775 41. **Peng C-K, Mietus JE, Liu Y, Lee C, Hausdorff JM, Stanley HE, Goldberger**
776 **AL & Lipsitz LA.** Quantifying fractal dynamics of human respiration: age and gender
777 effects. *Ann Biomed Eng* 30: 683–692, 2002.
778
- 779 42. **Pethick J, Winter SL, Burnley M.** Fatigue reduces the complexity of knee
780 extensor torque fluctuations during maximal and submaximal intermittent isometric
781 contractions in man. *J Physiol* 593: 2085-2096, 2015.
782
- 783 43. **Pincus SM.** Approximate entropy as a measure of system complexity. *Proc Nat*
784 *Acad Sci* 88: 2297-2301, 1991.
785
- 786 44. **Pincus SM.** Greater signal regularity may indicate increased system isolation. *Math*
787 *Biosci* 122: 161-181, 1994.
788
- 789 45. **Place N, Bruton JD, Westerblad H.** Mechanisms of fatigue induced by
790 isometric contractions in exercising humans and in mouse isolated single
791 muscle fibres. *Clin Exp Pharmacol Physiol* 36: 334–339, 2009.
792
- 793 46. **Poole DC, Ward SA, Gardner GW, Whipp BJ.** Metabolic and respiratory profile
794 of the upper limit for prolonged exercise in man. *Ergonomics* 31: 1265-1279, 1988.
795

- 796 47. **Poole DC, Ward SA, Whipp BJ.** The effects of training on the metabolic and
797 respiratory profile of high-intensity cycle ergometer exercise. *Eur J Appl Physiol* 59:
798 421-429, 1990.
799
- 800 48. **Richman JS, Moorman JR.** Physiological time-series analysis using approximate
801 and sample entropy. *Am J Physiol Heart Circ Physiol* 278, H2039-H2049, 2000.
802
- 803 49. **Saugen E, Vøllestad NK.** Metabolic heat production during fatigue from voluntary
804 repetitive isometric contractions in humans. *J Appl Physiol* 81: 1323-1330, 1996.
805
- 806 50. **Seely AJE, Macklem P.** Fractal variability: An emergent property of complex
807 dissipative systems. *Chaos* 22: 013108, 2012.
808
- 809 51. **Sejdić E, Lipsitz LA.** Necessity of noise in physiology and medicine. *Comput*
810 *Methods Programs Biomed* 111: 459-470, 2013.
811
- 812 52. **Slifkin AB, Newell KM.** Noise, information transmission, and force variability. *J*
813 *Exp Psych* 25: 837-851, 1999.
814
- 815 53. **Sosnoff JJ, Newell KE.** Age-related loss of adaptability to fast time scales in motor
816 variability. *J Gerontol* 63: 344-352, 2008.
817
- 818 54. **Sosnoff JJ, Vaillancourt DE, Newell KM.** Aging and rhythmical force output: loss
819 of adaptive control of multiple neural oscillators. *J Neurophysiol* 91: 172-181, 2004.
820
- 821 55. **Sturman MM, Vaillancourt DE, Corcos DM.** Effects of aging on the regularity of
822 physiological tremor. *J Neurophysiol*, 93: 3064-3074, 2005.

823

824 56. **Svendsen JH, Madeleine P.** Amount and structure of force variability during short,
825 ramp and sustained contractions in males and females. *Hum Mov Sci* 29: 35-47, 2010.

826

827 57. **Taylor AM, Christou EA, Enoka RM.** Multiple features of motor-unit activity
828 influences force fluctuations during isometric contractions. *J Neurophysiol* 90: 1350-
829 1361, 2003.

830

831 58. **Vaillancourt DE, Newell KM.** The dynamics of resting and postural tremor in
832 Parkinson's disease. *Clin Neurophysiol* 111: 2046-2056, 2000.

833

834 59. **Vaillancourt DE, Newell KM.** Ageing and the time and frequency structure of
835 force output variability. *J Appl Physiol* 94: 903-912, 2003.

836

837 60. **Vanhatalo A, Fulford J, DiMenna F, Jones AM.** Influence of hyperoxia on
838 muscle metabolic responses and the power-duration relationship during severe-intensity
839 exercise in humans: a ³¹P magnetic resonance spectroscopy study. *Exper Physiol* 95:
840 528-540, 2010.

841

842 61. **Vøllestad NK, Wesche J, Sejersted OM.** Gradual increase in leg oxygen uptake
843 during repeated submaximal contractions in humans. *J Appl Physiol* 68: 1150-1156,
844 1990.

Table 1. Voluntary torque, peripheral and central fatigue parameters, and EMG responses to contractions below (50%CT and 90%CT) and above (S1-S4) the critical torque.

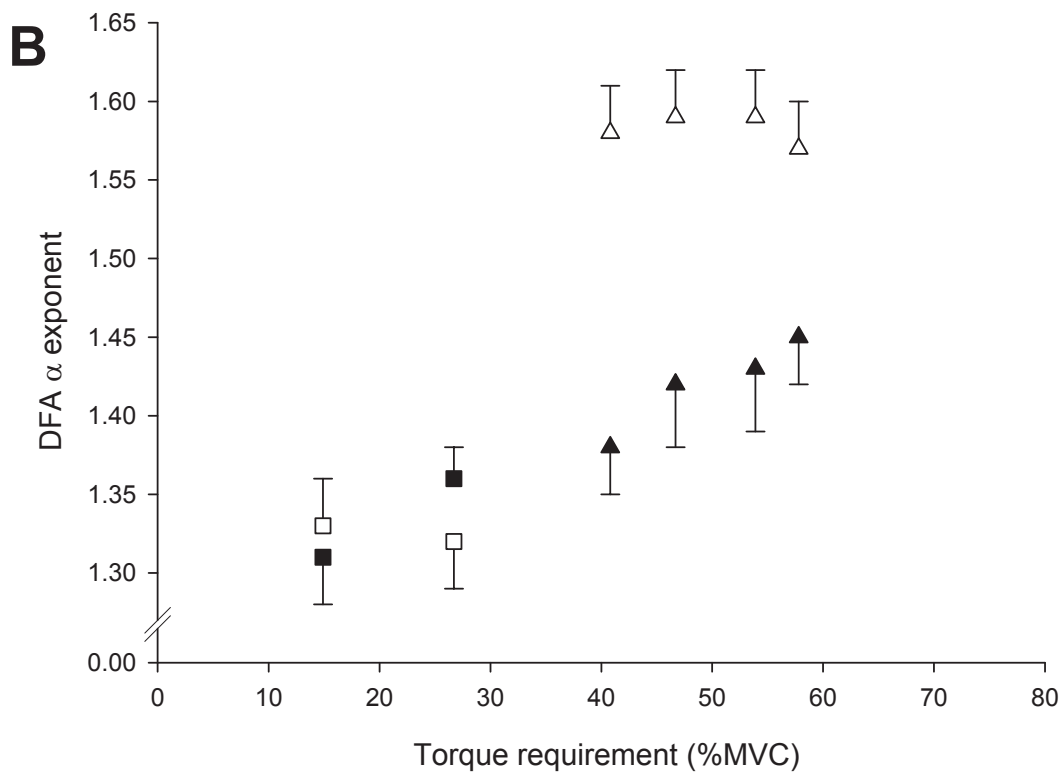
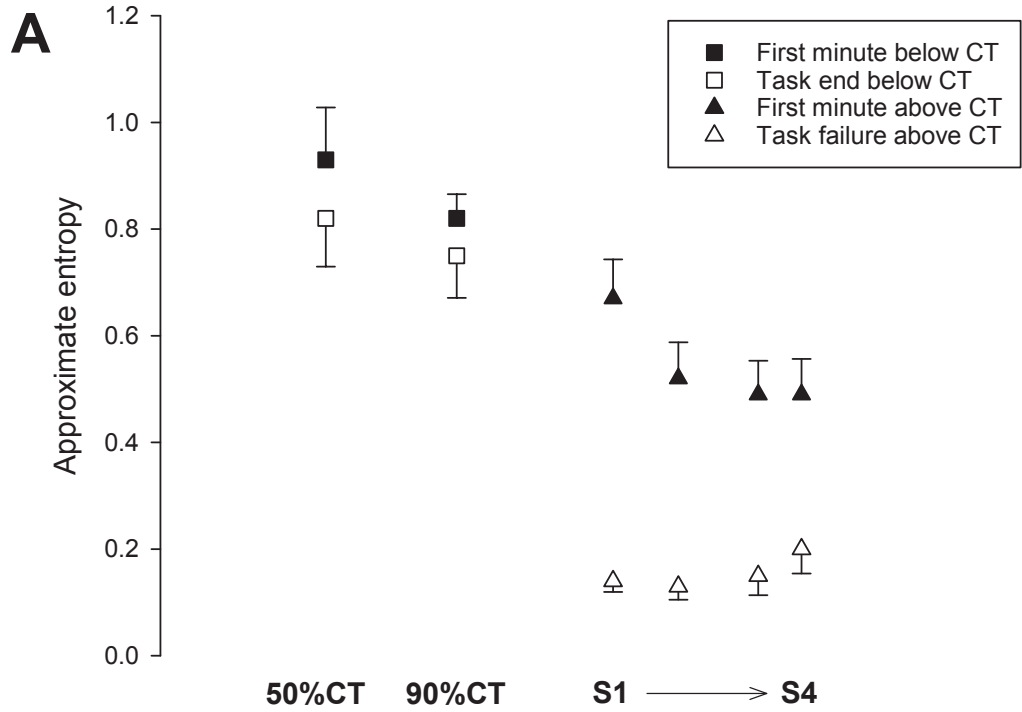
Parameter	50%CT	90%CT	S1	S2	S3	S4
Mean test torque, N.m	28.7 ± 2.3	51.7 ± 4.2	78.7 ± 6.3	89.7 ± 6.8	104.0 ± 8.4	112.7 ± 9.0
Mean test torque, ^a % MVC	14.9 ± 0.9	26.7 ± 1.6	40.8 ± 2.6	46.7 ± 3.2	53.9 ± 3.4	57.8 ± 2.5
Time to task end/failure, min	30.0 ± 0.0	30.0 ± 0.0	17.5 ± 1.3	8.1 ± 0.7	4.8 ± 0.5	2.9 ± 0.3
Global fatigue						
Pre-exercise MVC, N.m	226.2 ± 19.7	223.8 ± 21.8	199.9 ± 18.6	198.1 ± 17.2	200.6 ± 15.5	209.6 ± 19.2
Peak MVC at task end/failure, N.m	205.6 ± 18.6†‡	182.2 ± 19.5†‡	101.9 ± 8.2†	110.7 ± 9.7†	119.4 ± 10.2†	112.7 ± 8.0†
Mean MVC at task end/failure, N.m	180.5 ± 18.3*	162.1 ± 17.8*	77.7 ± 5.7	87.4 ± 8.1	101.0 ± 8.5	95.1 ± 7.6*
ΔMVC/Δt, N.m.min ⁻¹	-0.7 ± 0.1‡	-1.4 ± 0.3‡	-6.2 ± 1.3	-12.2 ± 1.8‡	-18.5 ± 3.2‡	-36.4 ± 5.5‡
Peripheral fatigue						
Pre-exercise doublet, N.m	97.2 ± 7.3	98.6 ± 8.5	95.1 ± 7.9	94.4 ± 8.7	92.3 ± 8.5	91.9 ± 7.7
Doublet at task end/failure, N.m	90.8 ± 6.9†‡	86.3 ± 7.6†‡	63.5 ± 4.9†	63.8 ± 8.1†	62.8 ± 5.0†	60.9 ± 6.3†
% Change at task end/failure	6.6 ± 1.3	12.5 ± 2.3	32.2 ± 3.8	32.6 ± 4.9	29.8 ± 5.2	32.7 ± 5.5
Δdoublet/Δt, N.m.min ⁻¹	-0.2 ± 0.05‡	-0.4 ± 0.1‡	-1.8 ± 0.4	-3.9 ± 0.7‡	-6.1 ± 1.3‡	-11.6 ± 2.5‡
Time to peak torque						
Pre-exercise, ms	91.3 ± 1.7	93.4 ± 2.4	95.4 ± 4.8	94.6 ± 4.5	94.9 ± 4.9	93.6 ± 2.8
At task end/failure, ms	92.1 ± 2.2	91.6 ± 2.5	86.8 ± 1.6	90.8 ± 3.2	91.9 ± 4.4	91.9 ± 2.2
One-half relaxation time						
Pre-exercise, ms	201.7 ± 31.7	162.3 ± 21.9	191.5 ± 27.5	179.6 ± 28.5	205.3 ± 26.4	215.6 ± 42.2
At task end/failure, ms	148.1 ± 27.4	135.0 ± 19.9	141.7 ± 19.8	125.9 ± 15.7	162.8 ± 21.3	168.0 ± 24.1
Central fatigue						
Pre-exercise VA, %	92.4 ± 0.5	93.6 ± 0.7	91.3 ± 0.9	91.5 ± 1.0	92.0 ± 1.3	92.4 ± 1.1
VA at task end/failure, %	91.2 ± 1.6‡	88.0 ± 1.3†	75.0 ± 3.2†	76.1 ± 1.1†	80.0 ± 1.7†	76.9 ± 3.7†
% Change at task end/failure	0.7 ± 0.7	6.0 ± 1.1	17.7 ± 3.6	16.7 ± 1.8	13.0 ± 1.5	16.7 ± 3.8
ΔVA/Δt, %/min	-0.04 ± 0.04‡	-0.2 ± 0.04	-0.9 ± 0.2	-2.1 ± 0.3‡	-2.7 ± 0.4‡	-5.3 ± 1.0‡
Surface EMG						
arEMG at task beginning, % MVC	13.8 ± 1.1	22.2 ± 2.3	35.2 ± 3.1	44.9 ± 4.9	53.7 ± 4.9	61.7 ± 4.3
arEMG at task end/failure, % MVC	14.9 ± 1.3	29.4 ± 4.4	62.4 ± 7.1†	70.1 ± 8.4†	76.5 ± 8.2†	77.6 ± 7.0†
ΔarEMG/Δt, % MVC/min	0.04 ± 0.02‡	0.2 ± 0.1‡	1.6 ± 0.4	3.5 ± 0.9	4.9 ± 1.5	5.4 ± 1.7

Values are means ± SEM. EMG, electromyogram; 50%CT and 90%CT, 50 and 90% of the critical torque, respectively; MVC, maximal voluntary contraction; Δ, change; t, time; VA, voluntary activation; arEMG, average rectified EMG of the vastus lateralis; ^aMean test torque is expressed as a percentage of the peak torque measured during the MVCs in visit 2. Letters indicate a statistically significant difference compared to the following: *mean test torque, †pre-exercise value/value at task beginning, ‡Severe 1.

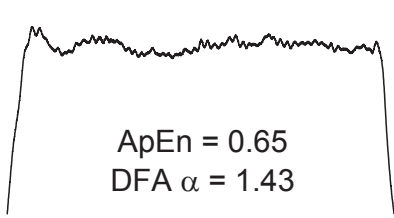
Table 2. Variability, complexity and fractal scaling responses to contractions below (50%CT and 90%CT) and above (S1-S4) the critical torque.

Parameter	50%CT	90%CT	S1	S2	S3	S4
SD						
SD at task beginning, N.m	0.9 ± 0.1	1.3 ± 0.1	2.0 ± 0.1	2.4 ± 0.2	2.8 ± 0.3	3.2 ± 0.3
SD at task end/failure, N.m	1.1 ± 0.2†	1.7 ± 0.2†	7.6 ± 0.4*	8.4 ± 0.8*	8.5 ± 1.4*	7.1 ± 0.8*
ΔSD/Δt, N.m.min ⁻¹ ^a	0.007 ± 0.003†	0.01 ± 0.003†	0.3 ± 0.03	0.8 ± 0.1	1.4 ± 0.4	1.6 ± 0.4
CV						
CV at task beginning, %	3.2 ± 0.2	2.5 ± 0.2	3.0 ± 0.1	3.0 ± 0.2	3.0 ± 0.3	3.0 ± 0.3
CV at task end/failure, %	4.3 ± 0.4†	3.0 ± 0.2†	11.0 ± 1.0*	11.0 ± 1.0*	9.0 ± 1.0*	7.0 ± 0.1*
ΔCV/Δt, %.min ⁻¹	0.03 ± 0.01†	0.02 ± 0.01†	0.5 ± 0.04	1.0 ± 0.2	2.0 ± 0.4	2.0 ± 0.5
Force accuracy (RMS error)						
RMS error at task beginning, N.m	2.8 ± 0.6	2.5 ± 0.3	2.7 ± 0.24	3.2 ± 0.3	4.4 ± 0.4	3.9 ± 0.4
RMS error at task end/failure, N.m	2.7 ± 0.5†	3.0 ± 0.5†	9.4 ± 0.5*	11.2 ± 1.2*	11.9 ± 1.7*	11.0 ± 0.9*
ΔRMS error/Δt, N.m.min ⁻¹ ^a	-0.003 ± 0.01†	0.01 ± 0.01†	0.4 ± 0.02	0.5 ± 0.1	1.4 ± 0.3	2.6 ± 0.3†
ApEn						
ApEn at task beginning	0.93 ± 0.07	0.82 ± 0.03	0.67 ± 0.06	0.52 ± 0.05	0.49 ± 0.05	0.49 ± 0.05
ApEn at task end/failure	0.80 ± 0.07†	0.75 ± 0.06†	0.14 ± 0.01*	0.13 ± 0.02*	0.15 ± 0.04*	0.20 ± 0.03*
ΔApEn/Δt ^a	-0.004 ± 0.002†	-0.002 ± 0.002†	-0.03 ± 0.01	-0.05 ± 0.01	-0.07 ± 0.01†	-0.11 ± 0.01†
DFA α						
DFA α at task beginning	1.31 ± 0.02	1.36 ± 0.01	1.38 ± 0.03	1.42 ± 0.03	1.43 ± 0.03	1.45 ± 0.03
DFA α at task end/failure	1.34 ± 0.03†	1.32 ± 0.03†	1.58 ± 0.01*	1.59 ± 0.02*	1.59 ± 0.02*	1.57 ± 0.03*
ΔDFA α /Δt ^a	0.001 ± 0.001†	-0.001 ± 0.001†	0.01 ± 0.002	0.02 ± 0.005	0.04 ± 0.01†	0.05 ± 0.01†

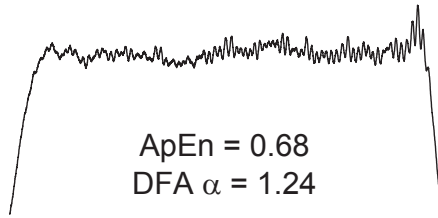
Values are means ± SEM. 50%CT and 90%CT, 50 and 90% of the critical torque, respectively; Δ, change; t, time; SD, standard deviation; CV, coefficient of variation; RMS error, root mean squared error vs. the target torque; ApEn, approximate entropy; DFA α, detrended fluctuation analysis. Letters indicate a statistically significant difference compared to the following: *pre-exercise value/value at task beginning, †Severe 1. ^aDue to the duration of some trials, discrimination between conditions at 2 decimal places is not possible. Therefore these data are expressed to 2 decimal places or the first significant figure as required.



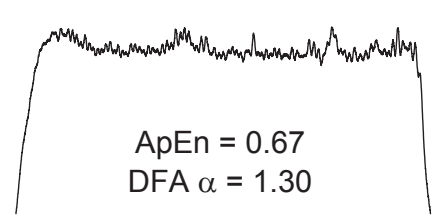
A



First minute

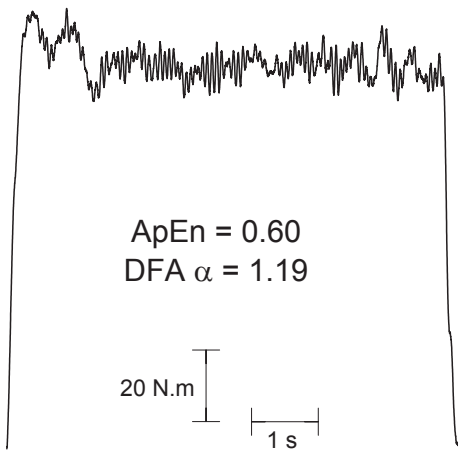


Mid-point

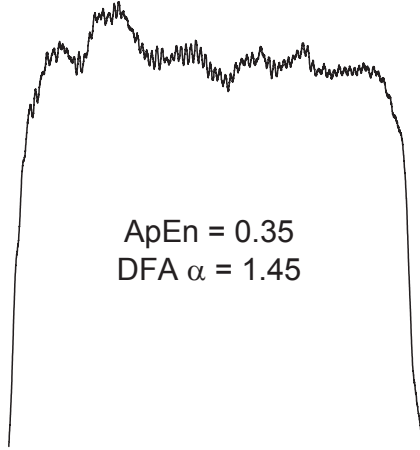


Task end/failure

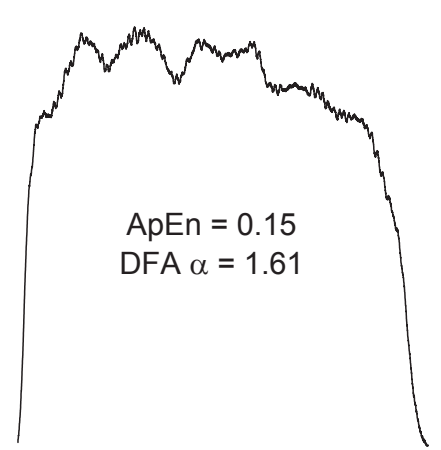
B



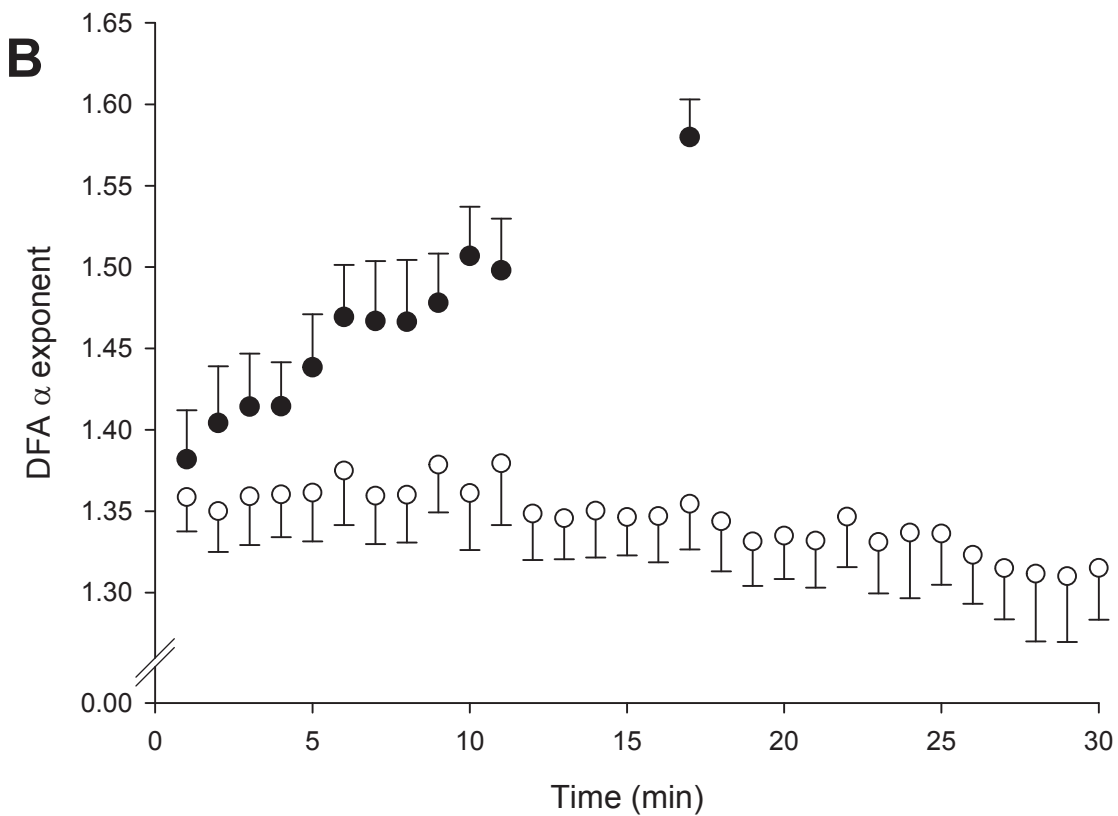
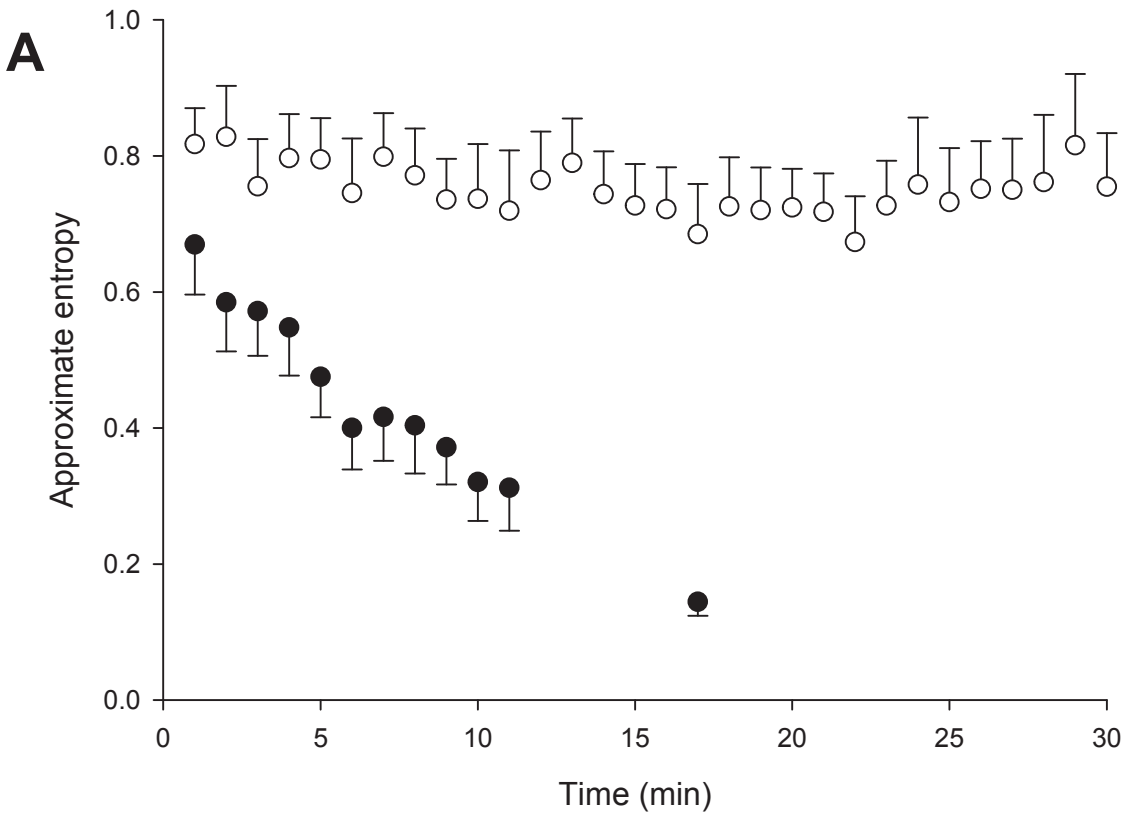
ApEn = 0.60
DFA α = 1.19

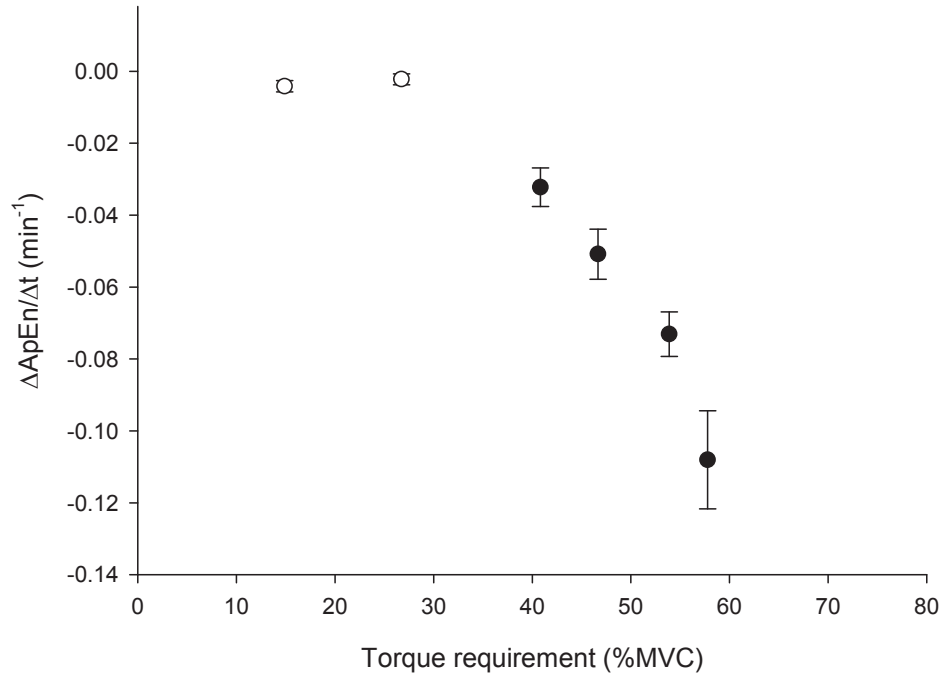


ApEn = 0.35
DFA α = 1.45



ApEn = 0.15
DFA α = 1.61



A**B**